Electronic Supplementary Material (ESI) for Energy & Environmental Science

Supplementary information

Formamidinium lead trihalide: a broadly tunable perovskite for efficient planar heterojunction solar cells

Giles E. Eperon, Samuel D. Stranks, Christopher Menelaou, Michael B. Johnston, Laura M. Herz and Henry J. Snaith

Department of Physics, University of Oxford, Clarendon Laboratory, Parks Road, Oxford, OX1 3PU, UK

1. Methods and Materials

Materials. Unless otherwise stated, all materials were purchased from Sigma-Aldrich or Alfa Aesar and used as received. Spiro-OMeTAD was purchased from Borun Chemicals.

Perovskite precursor synthesis: Formamidinium iodide (FAI) and formamidinium bromide (FABr) were synthesised by dissolving formamidinium acetate powder in a 2x molar excess of 57%w/w hydroiodic acid (for FAI) or 48%w/w hydrobromic acid (for FABr). After addition of acid the solution was left stirring for 10 minutes at 50°C. Upon drying at 100°C, a yellow-white powder is formed. This was then washed with diethyl ether and recrystallized twice with ethanol, to form white needle-like crystals. Before use, it was dried overnight in a vacuum oven.

To form $FAPbI_3$ and $FAPbBr_3$ precursor solutions, FAI and PbI_2 or FABr and $PbBr_2$ were dissolved in anhydrous N,N-dimethylformamide (DMF) in a 1:1 molar ratio, at 0.88M of each reagent, to give a 0.88M perovskite precursor solution. To form the $FAPbI_{3y}Br_{3(1-y)}$ perovskite precursors, mixtures were made of the $FAPbI_3$ and $FAPbBr_3$ solutions in the required ratios.

$CsPbI_3$ precursor was prepared by dissolving equimolar amounts of CsI and PbI_2 in dimethyl sulfoxide at 0.6M, in a nitrogen-filled glovebox. Films were spin-coated at 2000rpm and annealed at 100°C for 5 minutes in the glovebox.

$MAPbI_3$ precursor was prepared by dissolving equimolar amounts of methylammonium iodide (synthesised according to a literature procedure)[1] and PbI_2 in DMF at 0.88M, in a nitrogen-filled glovebox. Films were spin-coated at 2000rpm and annealed at 100°C for 5 minutes in the glovebox.

Film formation: For uniform and continuous film formation of $FAPbI_3$, just before spin-coating, 60µl of hydroiodic acid (57%w/w) was added to 1ml of the 0.88M precursor solution. To form films for optical characterisation and device fabrication, the $FAPbI_3$ precursor was diluted down to 0.55M with DMF.

For the $FAPbI_{3y}Br_{3(1-y)}$ samples for optical measurements, precursors were used as is, and spin-coated and annealed on glass in a nitrogen-filled glovebox at 170°C for 25 minutes.

For the time-resolved photoluminescence samples of $FAPbI_3$, the 0.55M precursor with added HI was spin-coated on clean glass substrates in a nitrogen-filled glovebox at 2000rpm. The films were then annealed in air at 170°C for 10 minutes. This gave very uniform layers ~400 nm thick of $FAPbI_3$. For the non-quenching sample, 10mg/ml PMMA in chlorobenzene was spin-coated on top of the perovskite at 1000rpm. For the quenching samples, 30mg/ml PCBM and 50mg/ml Spiro-OMeTAD were spin-coated on top of the perovskite at 1000rpm and 2000rpm respectively.

Substrate Preparation: Devices were fabricated on fluorine-doped tin oxide (FTO) coated glass (Pilkington, $7\Omega\ \square^{-1}$). Initially FTO was removed from regions under the anode contact by etching the FTO with 2M HCl and zinc powder. Substrates were then cleaned sequentially in hallmanex detergent, acetone, propan-2-ol and oxygen plasma. A ~50nm hole-blocking layer of compact TiO_2 was deposited by spin-coating a mildly acidic solution of titanium isopropoxide in ethanol (350ul in 5ml ethanol with 0.013M HCl) at 2000rpm, and annealed at 500°C for 30 minutes.

Perovskite Solar Cell Fabrication: To form the $FAPbI_3$ layer, the 0.55M precursor with added HI was spin-coated in a nitrogen-filled glovebox at 2000rpm, on a substrate heated to 85°C. The films were then annealed in air at 170°C for 10 minutes. This gave a very uniform layer ~400nm thick of $FAPbI_3$.

For $FAPbI_{3y}Br_{3(1-y)}$ devices, these were fabricated in the same way, by diluting precursor solutions down to 0.55M and adding a mixture of HI and HBr in the required ratio to maintain the correct iodide/bromide fraction.

The hole-transporting layer was then deposited via spin-coating a 0.788M solution in chlorobenzene of 2,2',7,7'-tetrakis-(N,N-di-p-methoxyphenylamine)9,9'-spirobifluorene (spiro-OMeTAD), with additives of 0.0184 lithium bis(trifluoromethanesulfonyl)imide (added in 0.61M acetonitrile solution) and 0.0659M 4-tert-butylpyridine. Spin-coating was carried out in air at 2000rpm.

Gold electrodes were thermally evaporated under vacuum of ~10^{-6} Torr, at a rate of ~0.1nm/s, to complete the devices.

Device characterisation: The current density–voltage (J-V) curves were measured (2400 Series SourceMeter, Keithley Instruments) under simulated AM 1.5 sunlight at 100 $mWcm^{-2}$ irradiance generated by an Abet Class AAB sun 2000 simulator, with the intensity calibrated with an NREL calibrated KG5 filtered Si reference cell. The mismatch factor was calculated to be 1.2% between 400 and 1100nm.[2] The solar cells were masked with a metal aperture to define the active area, typically 0.0625cm^{-2} and measured in a light-tight sample holder to minimize any edge effects.

External Quantum Efficiency measurements: External quantum efficiency was measured via fourier-transform photocurrent spectroscopy, a fast and sensitive spectral characterization method.[3] This was carried out using the modulated beam of a Bruker Vertex 80v Fourier Transform Interferometer with tungsten lamp source and a Stanford Research SR570 current preamplifier. Samples were calibrated to a Newport-calibratedreference silicon solar cell with a known external quantum efficiency. The solar cells were masked with a metal aperture to define the active area, typically 0.0625cm^{-2}.

Optical measurements: Transmittance and reflectance spectra were collected with a Varian Cary 300 UV-Vis spectrophotometer with an internally coupled integrating sphere.

Materials Characterization: A Hitachi S-4300 field emission scanning electron microscope was used to acquire SEM images. Sample thicknesses were measured using a Veeco Dektak 150 surface profileometer. X-ray diffraction spectra were obtained from full devices with no evaporated electrodes, using a Panalytical X'Pert Pro x-ray diffractometer.

Photoluminescence measurements: Steady-state and time-resolved PL measurements were acquired using a time-correlated single photon counting (TCSPC) setup (FluoTime 300, PicoQuant GmbH). Film samples were photoexcited using a 507nm laser head (LDH-P-C-510, PicoQuant GmbH) pulsed at frequencies between 0.3-10MHz, with a pulse duration of 117ps and fluence of ~30nJ/cm^2. The PL was collected using a high resolution monochromator and hybrid photomultiplier detector assembly (PMA Hybrid 40, PicoQuant GmbH).

Diffusion modeling: The PL decay dynamics were modeled by calculating the number and distribution of excitations in the film $n(x,t)$ according to the 1-D diffusion equation,

$$\frac{\partial n(x,t)}{\partial t} = D\frac{\partial^2 n(x,t)}{\partial x^2} - k(t)n(x,t) \qquad \text{(S1)},$$

where *D* is the diffusion coefficient and *k(t)* is the PL decay rate in the absence of any quencher material.[4] The total decay rate, $k = 1/k_f + 1/k_{nr} = \beta\tau^{-\beta}t^{\beta-1}$, was determined by fitting a stretched exponential decay to the PL data measured from perovskite layers with PMMA and assumed independent of the capping material. The effect of the quenching layer was included by assuming that all excitons which reach the interface are quenched with unit efficiency (*n(L,t)=0*, where *x=0* at the glass/perovskite interface and *L* is the perovskite film thickness). As the excitation pulse was from the glass substrate side of the samples, the initial distribution of excitons was taken to be $n(x,0)=n_0 exp(-\alpha x)$, where $\alpha=A/L$ (absorbance at 507 nm / perovskite layer thickness). Any deviation from this distribution due to reflection of the laser pulse at the perovskite/quencher interface was assumed to be negligible. In order to calculate the diffusion length L_D, the diffusion coefficient was varied to minimize the reduced chi-squared value,

$$\chi_r^2 = \frac{1}{(n-p-1)}\sum\frac{\left(y(t)-y_c(t)\right)^2}{y(t)} \qquad \text{(S2)},$$

where *y(t)* and $y_c(t)$ are the measured and calculated PL intensities at time *t*, *n* is the number of data points and *p* is the number of fitting parameters.[5] The equation was solved numerically using the Crank-Nicholson algorithm and the number of excitons integrated across the entire film in order to determine the total PL intensity at time *t*. Both the stretched exponential and 1-D diffusion models were fit to the experimental TCSPC data by iterative reconvolution with the instrument response function (IRF) which was recorded separately, such that the observed PL intensity,

$$I(t) = \int g\,(t)f(t-t')dt' \qquad \text{(S3)},$$

is the result of the real decay curve,*f(t)*, convolved with the IRF, *g(t)*.[5] The diffusion length L_D is given by $L_D = \sqrt{D\tau}$, where $\tau = 1/k$ is the recombination lifetime in the absence of a quencher. The errors reported in the text account for errors in the fitting procedure and in sample thickness. The latter is approximated to be ±25nm.

2. Perovskite Tolerance Factor

The tolerance factor for a particular perovskite has been defined as:[6]

$$t = \frac{r_A + r_X}{\sqrt{2}(r_B + r_x)}$$

Where r_A, r_B, and r_X are the ionic radii of the A, B, and X components of the perovskite lattice. t = 1 would correspond to a perfectly packed structure, and it can be varied only in a restricted range. For most perovskites it has been stated to be between 0.8 and 0.9.[6] This then sets limits on the feasibility of particular A cation replacements, based on their ionic radius, whilst keeping the same B and X components in the lattice.

3. X-ray diffraction spectra for $FAPbI_yBr_{3-y}$

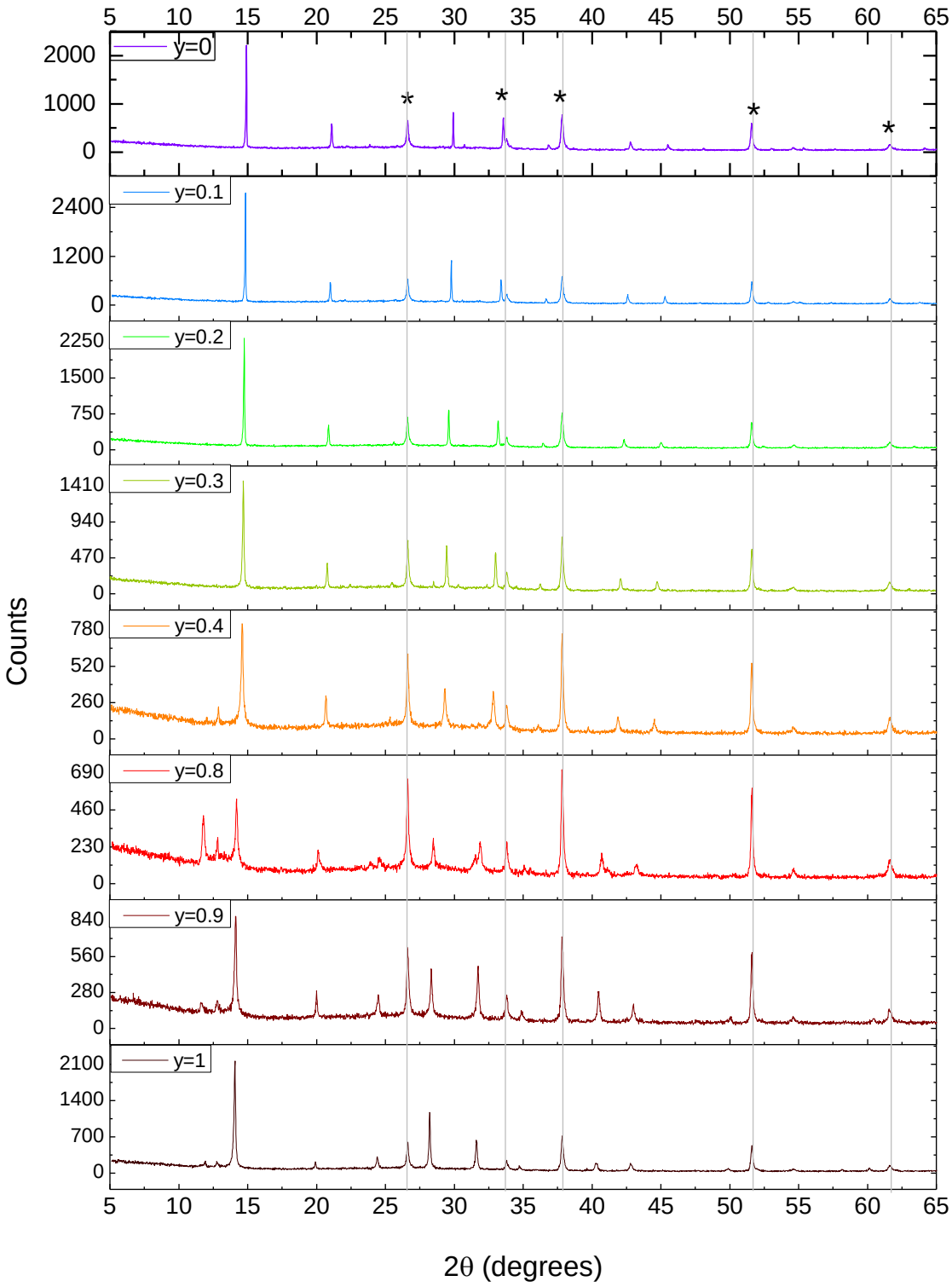

Fig. S1: *X-ray diffraction spectra for the whole range of $FAPbI_yBr_{3-y}$ perovskites formed, on fluorine-doped tin oxide-coated glass substrates. Peaks labelled with a * are assigned to the fluorine-doped tin oxide substrate.*

4. Pseudocubic lattice parameter calculation

Because the tetragonal phase is transitioned to from the cubic phase by a slight rotation of the adjacent PbX_6 octahedra, whilst maintaining corner-sharing, as shown in Fig. S2, we can define the tetragonal phase by a pseudocubic phase, where the (100) spacing in the pseudocubic system replaces the (110) tetragonal spacing, as previously described in the litreature.[7,8] The pseudocubic lattice parameters are then determined from lattice parameters **a** and **c** by:

$$\boldsymbol{a*} = \frac{\sqrt{2a^2}}{2} \; ; \; \boldsymbol{c*} = \frac{c}{2}$$

For a cubic lattice, **a*** and **c*** should be identical, so for the most accurate representation, we averaged between **a*** and **c*** determined in this way to get a single pseudocubic lattice parameter.

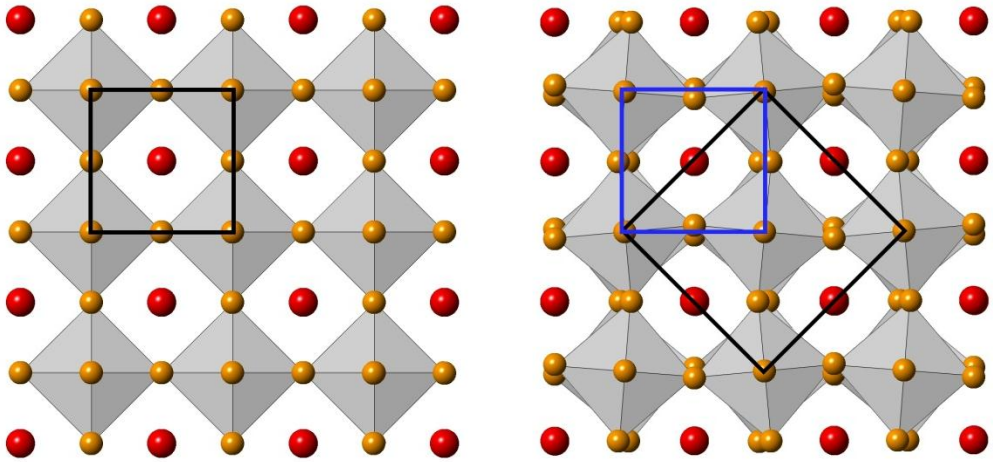

Fig. S2: *Cubic (left) and tetragonal (right) lattices formed by the $FAPbI_yBr_{3-y}$ perovskites. The unit cell is shown in black. The pseudocubic lattice in the tetragonal configuration is shown in blue. Red = A cation, yellow = halide, grey tetrahedra are centred on the metal cation.*

5. Tauc plot bandgap calculation

Bandgap was determined by plotting $(\alpha h\nu)^2$ against energy in eV, known as a Tauc plot.[9] This assumes the compounds have a direct bandgap. The estimated bandgap is determined from the extrapolation of the linear region to the energy-axis intercept. Absorption coefficient α was determined from absorption spectra collected with an integrating sphere. An example absorption spectrum and Tauc plot are shown below.

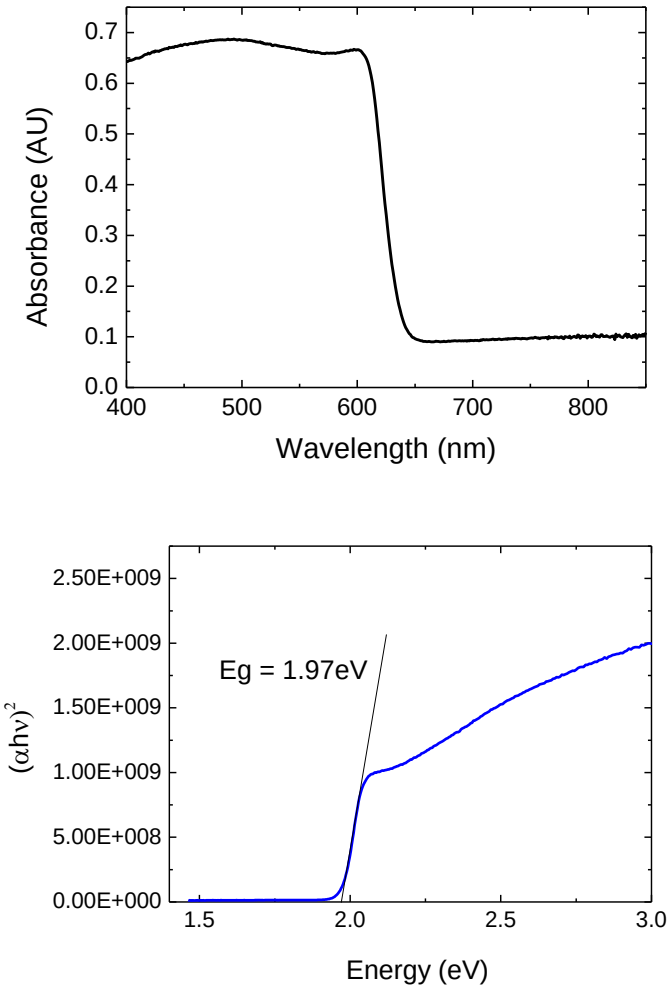

Fig. S3: top, *absorbance spectrum of a $FAPbI_yBr_{3-y}$ perovskite (where y=0.3).* ***bottom,*** *Tauc plot assuming direct bandgap, showing determination of estimated bandgap from intercept.*

6. XRD spectrum of $FAPbI_3$ film

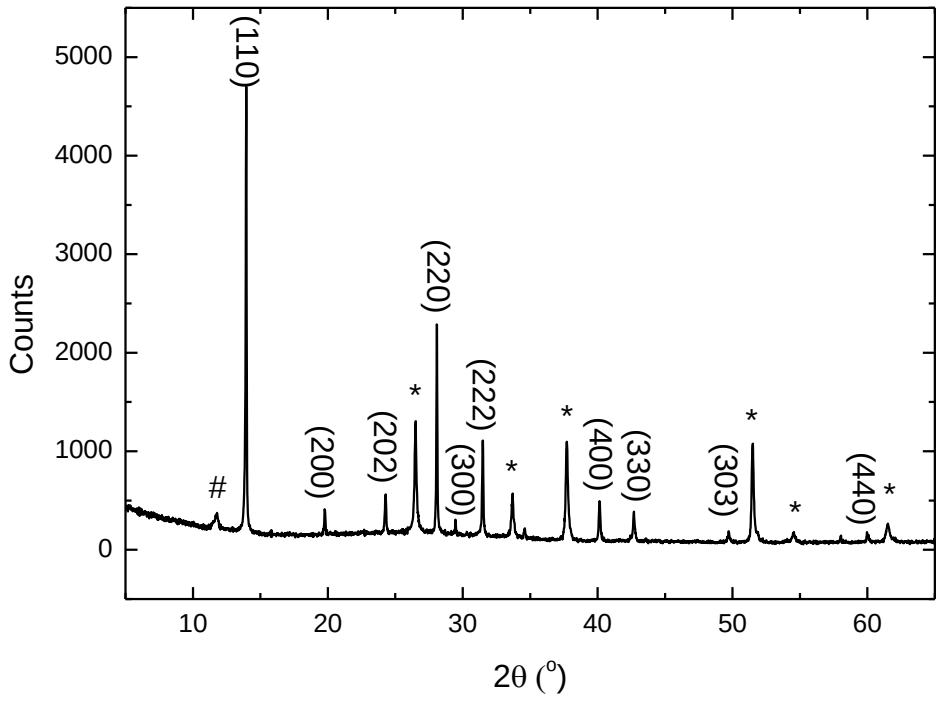

Fig. S3: *X-ray diffraction spectrum for a smooth and continuous $FOPbI_3$ film such as those used in the high-efficiency devices and quenching films. Peaks labelled with a * are assigned to the fluorine-doped tin oxide substrate, those with a # to PbI_2 impurities, and other peaks are assigned to the labelled reflections from a tetragonal perovskite lattice with unit cell parameters **a**=**b**=8.99Å, **c**=11.0Å, in good agreement with the previous report on $FAPbI_3$*[10]

7. Photoluminescence quenching: steady-state photoluminescence and absorption

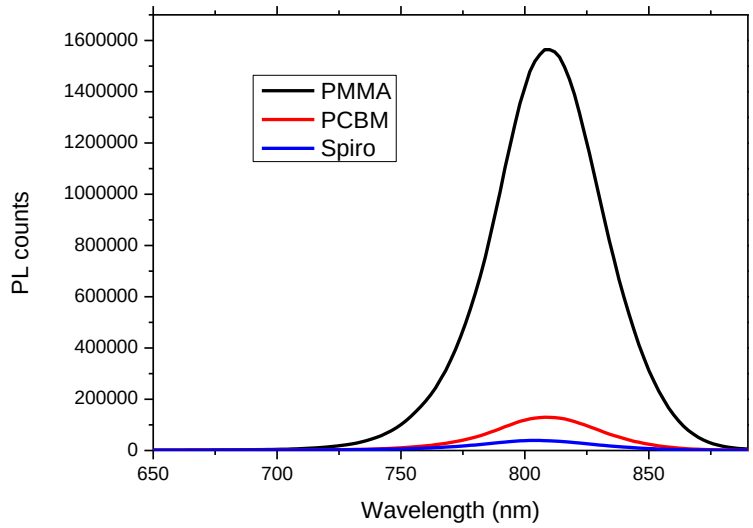

Fig. S4: *Steady-state photoluminescence spectra of a $FAPbI_3$ film of 400nm thickness coated in either an inert layer of polymethylmethacrylate (PMMA), the electron-quenching layer phenyl-C61-butyric acid methyl ester (PCBM), and the hole-quenching layer spiro-OMeTAD, demonstrating effective photoluminescence quenching for both holes and electrons with these layers.*

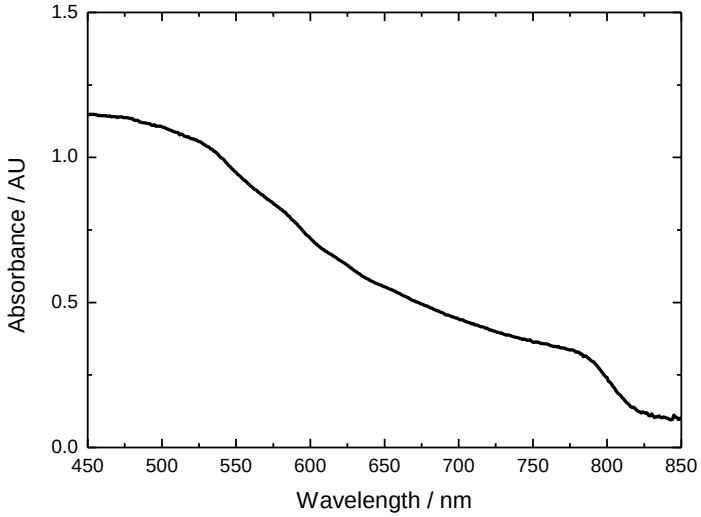

Fig. S5: *Absorption spectrum of a 400nm thin film of $FAPbI_3$.*

8. Statistics for whole batch of optimised $FAPbI_3$ solar cells

No. cells	J_{sc} ($mAcm^{-2}$)	V_{oc} (V)	FF	PCE (%)
24	18.8±3.3	0.85±0.08	0.60±0.09	9.7±2.6

Table ST1: *Device statistics from a batch of 24 individual devices prepared using the optimised fabrication procedure, extracted from current-voltage characteristics measured under 100mWcm^{-2} AM1.5 illumination. Errors are calculated from the standard deviation in the batch.*

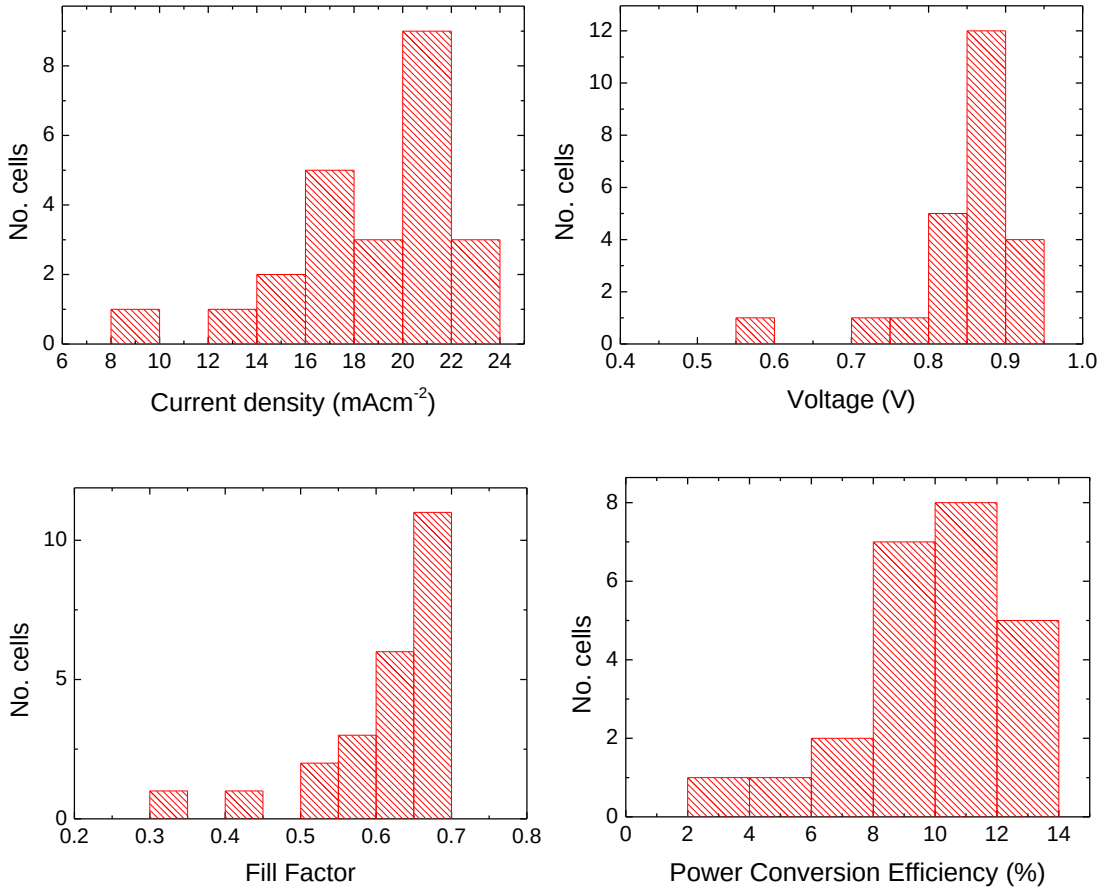

Fig. S6: *Histogram representation of the solar cell characteristics for the same batch of optimised devices.*

9. Degradation of FAPbI3 and MAPbI3

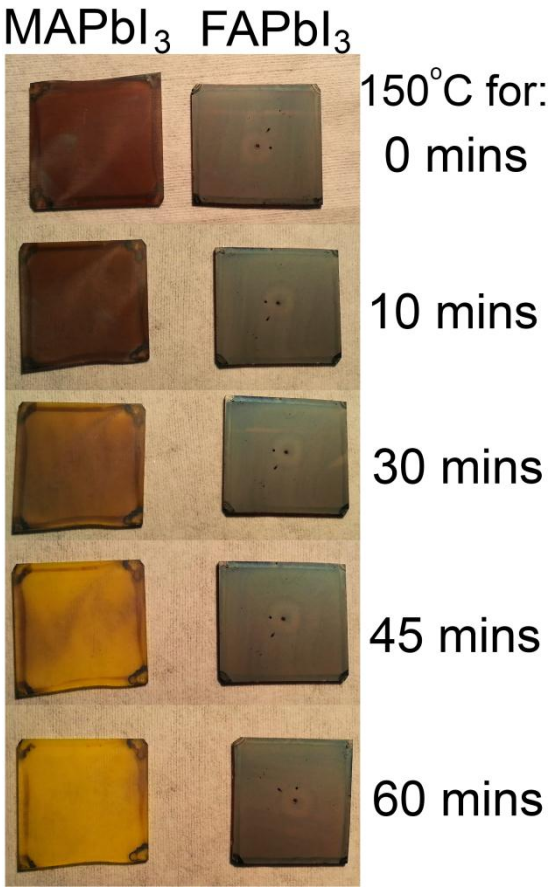

Fig. S7: *Thermal degradation of MAPbI3 and FAPbI3, when bare spin-coated films of each perovskite are heated in air at 150°C for the times indicated.The yellow colour that the $MAPbI_3$ degrades to is lead iodide (verified by XRD, not shown).*

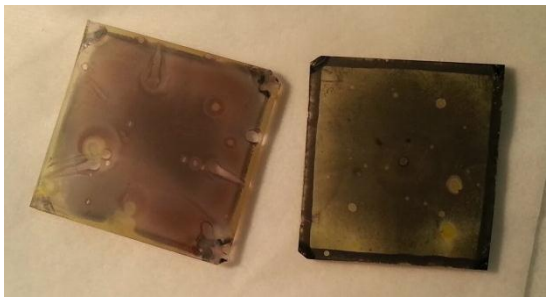

Fig. S8: *Films of $MAPbI_3$ (left)and $FAPbI_3$ (right) upon exposure to a close to 100% relative humidity atmosphere for ~15 minutes at room temperature. The atmosphere was created by pouring water onto a tissue in a sealed glass container with the films. Degradation is evident at an approximately equal rate in both films.*

References

1. M. M. Lee, J. Teuscher, T. Miyasaka, T. N. Murakami, and H. J. Snaith, *Science*, 2012, **338**, 643.

2. H. J. Snaith, *Energy Environ. Sci.*, 2012, **5**, 6513.

3. K. Vandewal, L. Goris, I. Haeldermans, M. Nesládek, K. Haenen, P. Wagner, and J. V. Manca, *Thin Solid Films*, 2008, **516**, 7135–7138.

4. P. E. Shaw, A. Ruseckas, and I. D. W. Samuel, *Adv. Mater.*, 2008, **20**, 3516–3520.

5. J. R. Lakowicz, *Principles of Flurescence Spectroscopy*, Spinger London Ltd, 2007.

6. D. B. Mitzi, *Progress in Inorganic Chemistry, Volume 48*, John Wiley & Sons, Inc, 1999.

7. D. L. Proffit, H. W. Jang, S. Lee, C. T. Nelson, X. Q. Pan, M. S. Rzchowski, and C. B. Eom, *Appl. Phys. Lett.*, 2008, **93**, 111912.

8. J. H. Noh, S. H. Im, J. H. Heo, T. N. Mandal, and S. Il Seok, *Nano Lett.*, 2013, **13**, 1764–1769.

9. J. Tauc, R. Grigorovici, and a. Vancu, *Phys. Status Solidi*, 1966, **15**, 627–637.

10. C. C. Stoumpos, C. D. Malliakas, and M. G. Kanatzidis, *Inorg. Chem.*, 2013, **2**.